Sulfation Mechanism and Catalytic Behavior of Manganese Oxide in the Oxidation of Methanethiol

Caroline M. Cellier, Valérie Vromman, Valérie Ruaux, Eric M. Gaigneaux,* and Paul Grange†

Unité de catalyse et chimie des matériaux divisés, Université catholique de Louvain, Croix du Sud, 2/17, B-1348 Louvain-la-Neuve, Belgium

Received: February 25, 2004; In Final Form: April 29, 2004

This work studies the behavior of a manganese dioxide catalyst during the total oxidation of methanethiol. Modifications of the working γ-MnO_2 catalyst were characterized by XPS, XRD, DRIFTS, and potentiometric measurements after reactions at different durations and at different temperatures. At temperatures below 200 °C, sulfur adsorbs on γ-MnO_2 in the form of sulfate species and poisons CH_3SH adsorption sites. Accordingly, the methanethiol conversion is strongly inhibited. At higher temperatures (260−280 °C), γ-MnO_2 is strongly reduced and is converted to a moderately active manganese sulfate phase while the reaction proceeds. This contribution also shows that the activity and selectivity of the manganese sulfate phase formed in situ at high temperature are comparable to those of a commercial manganese sulfate. The variation of the reaction temperature between 280 and 150 °C controls the reversible hydration/dehydration of the manganese sulfate phase and its associated activation/deactivation. This important change in activity is accompanied by a change in the main byproduct formation. At 280 °C, the dehydrated manganese sulfate phase is fairly active and favors the production of dimethyl disulfide. On the contrary, the hydrated phase that exists only in the lower-temperature region is much more reactive and promotes the production of methanol.

I. Introduction

It is now well established that transition-metal oxides are effective catalysts for the total oxidation of volatile organic compounds.[1,2] In particular, γ-MnO_2 is a very promising catalyst that is more active than conventional catalysts based on noble metals.[3] Moreover, the low toxicity and low cost of manganese oxides have largely contributed to their integration into commercial systems and continuous study by many research groups.[3−10]

However, the wide range of emitted VOCs includes organic sulfur-containing compounds such as mercaptans and (di)-sulfides. In the presence of sulfur-containing compounds, oxide catalysts usually deactivate by the incorporation of sulfur.[8−13] The main mechanisms of sulfur deactivation are (i) poisoning by sulfur adsorption on active sites and (ii) interactions of sulfur with the catalyst that induces its structural modifications.[13−15] Manganese oxides are also very sensitive to the presence of sulfur, leading to the formation of manganese sulfate.[8,9,16,17] Gandia et al.[4,18] showed that the impregnation of sulfates on Mn_2O_3-based catalysts decreases their activity in the complete oxidation of ketones. Ferrandon et al.[8] also reported that the activity of a MnO_x catalyst in the oxidation of carbon monoxide and VOCs is poisoned after exposure to SO_2. Heyes et al.[16] have nevertheless shown that a MnO_2 catalyst remains moderately active in the oxidation of VOCs despite the fact that some manganese sulfate phases were detected at the end of the life test at 400 °C. In a complementary study, the same authors also reported that $MnSO_4$ is active in the removal of methanethiol above 300 °C.[19] Recently, we have shown that manganese sulfate is indeed an active catalyst in this reaction at lower temperature (150 °C) but only if it is stabilized in its hydrated $MnSO_4 \cdot H_2O$ form.[20] We also demonstrated that the reaction temperature dictates the reversible hydration/dehydration of the manganese sulfate phase and its subsequent activation/deactivation. In the same order of ideas, Wang and Weng[21,22] reported that the impregnation of sulfate groups on CuO/Al_2O_3 enhances its acidity and activity toward the total oxidation of dimethyl disulfide. Also, the high activities of sulfated metal oxides in low-temperature complete oxidations of propane have been established by Ishiwaka et al.[23] Thus, there is contradictory information regarding the effect of sulfate groups on the activity, which seems to depend on the nature of the catalyst and on the reaction.

Furthermore, the conditions of sulfate formation and the nature of formed sulfate species, especially in the case of manganese sulfate, are not fully understood. On one hand, Otsuka et al.[24,25] showed that the reaction between SO_2 and MnO_2 produces surface or bulk sulfate species depending on the reaction temperature. On the other hand, Rosso et al.[26] postulated that the formation of manganese sulfate from manganese-containing perovskite materials was ruled out because of the low stability of manganese(III−IV) sulfates. However, Kijlstra et al.,[9] who studied the poisoning of MnO_x-supported catalysts by SO_2, showed that $MnSO_4$ formation was independent of the Mn oxidation state and the presence of oxygen. Their envisaged mechanism assumed that SO_2 reacts directly with oxidic manganese sites at moderate temperature.[9] In contrast, the sulfation mechanism proposed by Sultanov et al.[17] to explain the deactivation of metal oxides (including Mn_3O_4) in the oxidation of CO involved two steps: a conversion of SO_3 into H_2SO_4 in the presence of water, followed by the reaction between H_2SO_4 and the solid.

* To whom correspondence should be addressed. E-mail: gaigneaux@cata.ucl.ac.be. Tel: +32 10 47 36 65. Fax: +32 10 47 36 49. E.M.G. is research associate for the National Foundation for Scientific Research (FNRS) of Belgium.

† Deceased July 2003.

10.1021/jp049158m CCC: $27.50
Published on Web 06/03/2004

The difference in activity between deactivated (sulfated) manganese oxides and manganese sulfates is therefore a subject that is worth debating. As a continuation of the understanding of manganese sulfate behavior,[20] we now study the sulfation of a manganese dioxide catalyst in the oxidation of methanethiol. The behavior of a sulfated γ-MnO_2 sample is compared to that which we have recently reported for $MnSO_4 \cdot H_2O$. In this study, we present the results of tests performed with methanethiol at different temperatures and during a competition test performed with *n*-hexane and methanethiol. A comparison of the activity of MnO_2 and Mn_2O_3 is also made. The modifications undergone by the γ-MnO_2 catalyst under different reaction conditions are characterized by XRD, XPS, and potentiometric and DRIFTS analyses.

II. Experimental Section

1. Materials. The material solids used is this work are γ-MnO_2 (103 m^2/g) and Mn_2O_3 (30 m^2/g) samples provided by Erachem Europe S. A. (Tertre, Belgium) and a manganese sulfate monohydrate ($MnSO_4 \cdot H_2O$) sample purchased from Merck (ref 1.059999.1000; the specific surface area of this sample was impossible to measure, likely because of phase transformation occurring during the experiment).

2. Techniques of Characterization. XRD was performed on a Siemens D-5000 powder diffractometer using Cu $K\alpha_{1,2}$ radiation ($\lambda = 1.5418$ Å). The sample powders were mounted on silicon monocrystal sample holders. The 2θ range between 2 and 85° was scanned at a rate of 0.02°/s. Identification of the phases was carried out by using JCPDS database.[27]

XPS was performed with a SSI X-Probe (SSX-100/206) photoelectron spectrometer from Surface Science Instrument (Fisons) equipped with a microfocused Al Kα monochromatic X-ray source (1486.6 eV). Charge neutralization was achieved by using an electron flood gun adjusted at 10 eV and placing a nickel grid 3 mm above the sample. The pass energy for the analyzer was 50 eV, and the spot size was 1000 μm in diameter, corresponding to a fwhm of 1.1 eV for the Au $3d_{5/2}$ band of a gold standard. For these measurements, Mn 2p, Mn 3s, S 2p, O 1s, and C 1s bands were recorded. The binding energies were calculated, taking as a reference the *C*-(C, H) component of the C 1s adventitious carbon peak fixed at 284.8 eV. The spectra were decomposed with the least-squares fitting routine with a Gaussian/Lorentzian ratio of 85/15 and after subtracting a calculated baseline (Shirley type) (performed with CASA-XPS program). The atomic concentration ratios were calculated by normalizing the surface area ratio with sensivity factors based on Scoffield cross sections.

Potentiometric titrations of the manganese valence state were realized by the titration of Mn(IV) species in the sample and total manganese ions in the samples. These analyses were set up and performed at the R&D department of Erachem Europe S. A. (Manganese and Recycling Operations, Tertre, Belgium). Samples were first dissolved in an acidic solution of iron(II) ammonium sulfate that selectively reduces Mn^{4+} to Mn^{2+}. The excess ferrous ions (Fe^{2+}) were then titrated with a solution of $KMnO_4$ to determine the number of Mn^{4+} ions. The total amount of manganese present in the samples was then determined by adding hot hydrochloric acid to the solution to reduce all Mn ions to Mn^{2+}. The Mn^{2+} ions were then titrated with a solution of $KMnO_4$.

DRIFTS spectra were obtained by using a Brucker EQUINOX55 infrared spectrometer equipped with an air-cooled MIR source with KBr optics and an MCT detector. The powdered samples were placed on a dry KBr bed in the DRIFTS sample holder. The spectra (200 scans with 4 cm^{-1} resolution) were recorded in static air. They are presented in absorbance mode without any manipulation. The spectrum of dry powdered KBr was used as the background.

3. Activity Measurements. The oxidation of methanethiol (CH_3SH or MSH) was used to characterize the activity and deactivation of the catalysts. Methanethiol was chosen as a model compound of sulfur-containing volatile organic compounds because it has often be used in other studies dealing with the catalytic removal of S−VOCs[16,19,28−31]and because of its high volatility that makes it easily available in certified gaseous mixture. As in our previous work,[3,20] a concentration of 250 vppm of VOC (methanethiol) was used to perform the tests. The catalytic tests were performed in a fixed-bed flow microreactor at atmospheric pressure. For most of the tests, the reaction feed was a 100 mL min^{-1} flow made of a mixture of 250 vppm methanethiol (INDUGAS, certified mixture, 99.999%, 4950 vppm in N_2) and 20 vol % O_2 (INDUGAS, 99.995%) in N_2 (INDUGAS, 99.995%). The catalytic activity of the manganese oxide in the absence of sulfur-compounds was measured in a test with a flow of 100 mL min^{-1} composed of a mixture of 125 vppm *n*-hexane (INDUGAS, certified mixture, 99.999%, 5005 vppm *n*-hexane in N_2) and 20 vol % O_2 (INDUGAS, 99.995%) in N_2 (INDUGAS, 99.995%). A competition test was also performed with a mixture of 125 vppm of *n*-hexane, 250 vppm of methanethiol, and 20 vol % of O_2 in N_2. The catalytic tests were performed with 0.1 g of catalyst sieved between 0.2 and 0.315 mm. All of the catalytic tests were performed with a W/F ratio of 0.1 g catalyst per 100 mL/min of total flow, which corresponds to a space velocity of 72 000 h^{-1} (NTP) with MnO_2 and Mn_2O_3. The catalyst was diluted in approximately 7 cm^3 of glass beads of the same diameter (previously checked to be inactive). Before reaction, the catalysts were heated in situ at the reaction temperature under a pure oxygen flow (50 mL min^{-1}). Before measuring the conversion, we maintained the oxygen flow at the reaction temperature for 30 min. The activity of the catalysts was measured either during isothermal running at 150, 180, 220, 260 or 280 °C or after varying the temperature between 150 and 280 °C. The time on stream is always defined as the time at which the reactant feed is introduced into the reactor. The reactants and the products of incomplete oxidation were analyzed by on-line gas chromatography (Varian CP-3800 gas chromatograph with a capillary column of WCOT fused silica, 15 m × 0.32 mm i.d., coating CP-SIL 5 CB) and quantified using a flame ionization detector (FID). The activity results are expressed in term of methanethiol conversion calculated on the basis of its disappearance from the reactant flow. The yields of the two main detected organic products (methanol and dimethyl disulfide) were calculated as the ratio of their concentration measured at the outlet of the reactor to the concentration of methanethiol measured at the inlet of the reactor multiplied by the stoichiometric factor existing between the product and methanethiol (e.g., two molecules of methanethiol being needed to produce one molecule of dimethyl disulfide).

III. Results

III.1. Catalytic Activity Measurements. A series of catalyst tests with 250 vppm of CH_3SH were conducted to evaluate the activity and identify the sulfur poisoning effect on γ-MnO_2. Figure 1 shows the conversion of methanethiol obtained at five different temperatures as a function of time. The initial conversion was always equal to 100% at each temperature and was then followed by a more or less rapid and important

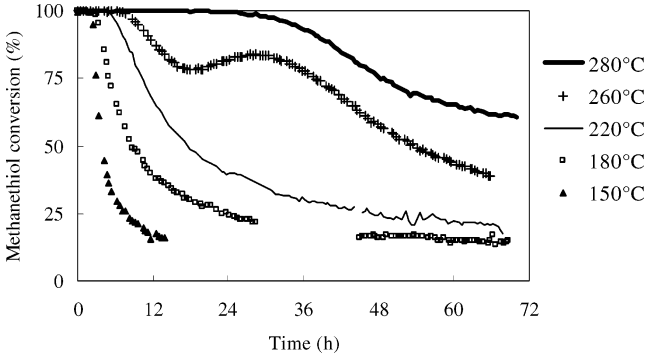

Figure 1. Conversion of 250 vppm of methanethiol as a function of time at different temperatures over a fresh γ-MnO_2 catalyst.

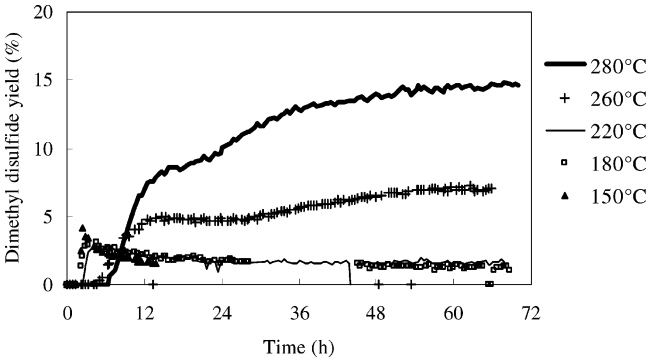

Figure 2. Dimethyl disulfide yield over fresh γ-MnO_2 in the oxidation of 250 vppm of CH_3SH at different reaction temperatures.

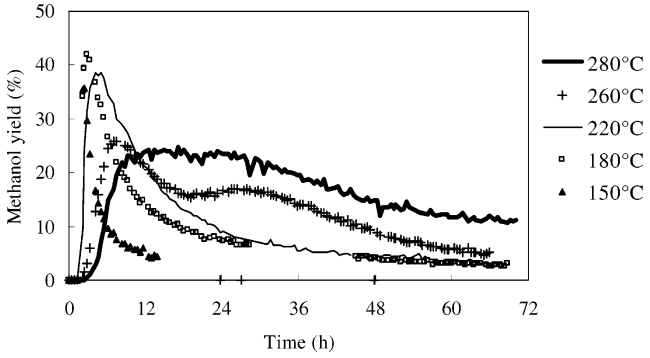

Figure 3. Methanol yield over fresh γ-MnO_2 produced during the oxidation of 250 vppm of CH_3SH at different reaction temperatures.

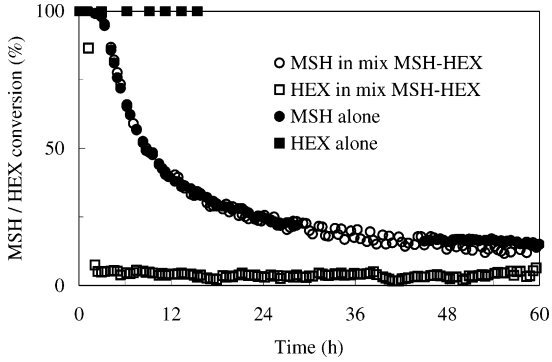

Figure 4. Conversion of 125 vppm of *n*-hexane (HEX) and 250 vppm of methanethiol (MSH) over γ-MnO_2 alone and in a mixture at 180 °C.

decrease in conversion. The deactivation rate appeared to decrease with increasing temperature. At 180 °C, the activity decrease started rapidly, and more than 75% conversion efficiency was lost during the first 24 h. However, at 280 °C, the total disappearance of the inlet methanethiol was maintained for 24 h before the conversion gradually decreased and then stabilized at around 60% after 3 days. The abnormal behavior observed in the conversion of methanethiol at 260 °C could be the consequence of a change in the catalyst occurring during the reaction. At this stage, one could, for example, envisage the occurrence of phenomena such as reduction, sulfation, and so forth or combination of them. This is further discussed in the following text. Complete conversion of the 250 vppm methanethiol can thus not be achieved in a stable way over γ-MnO_2 under any conditions and temperatures of reaction investigated here. After reaction at 150 °C for 15 h as well as after reaction at 260 °C, a decrease in the specific surface area in the range of 35 to 40 m^2/g was observed. (An accurate measurement of the surface areas was, however, not possible because of difficulties encountered in separating the catalyst from the glass beads.) To detect other catalyst changes, we performed characterizations of the catalyst after these reactions at different temperatures ; these are described below.

Another aspect concerns the products of the methanethiol oxidation. Dimethyl disulfide and methanol have been identified as the two main products of incomplete oxidation. Figures 2 and 3 present the yields of these two products as a function of time at different reaction temperatures. As shown in Figure 2, the yield of dimethyl disulfide increased with increasing reaction temperature. After more than 48 h, the yield of dimethyl disulfide appeared to be stable. Figure 3 shows that the production of methanol with respect to the time on stream and temperature was very different from the dimethyl disulfide formation. Methanol was detected at the reactor outlet after about 2 h of reaction. Then, yields rapidly increased to reach a maximum. The time to reach this maximum increased with increasing temperature, but the levels of the maxima appeared to decrease with increasing temperature. Thus, we note that whereas the formation of dimethyl disulfide increased with decreasing methanethiol conversion, decreasing methanol yield accompanied the loss of activity.

Figure 4 compares the conversion of 250 vppm methanethiol and 125 vppm *n*-hexane obtained when they are introduced alone or together in the feed. The experiments are conducted at 180 °C. This temperature was chosen because a total and stable oxidation of 125 vppm of *n*-hexane was measured at 180 °C when *n*-hexane is introduced without any methanethiol in the flow. Considering the mixture, it turns out that the evolution with the time on stream of the conversion of methanethiol was not modified by the presence of the *n*-hexane. On the contrary, the *n*-hexane conversion rapidly decreased below 10%. The conversion of *n*-hexane thus appeared strongly inhibited by the presence of methanethiol.

Figure 5 shows the activity and the yield of the main organic products measured on a more reduced manganese oxide sample (Mn_2O_3) compared with those of our reference manganese dioxide catalyst. The activity was measured at 150 °C as a function of the time on stream. The comparison was made at constant catalyst mass (0.1 g), meaning that difference areas of manganese oxide were exposed. Figure 5 shows that, under these conditions, Mn_2O_3 was less active than MnO_2 and lost its activity more quickly. However, this difference in surface area may not account for the difference in behavior discussed in this contribution, namely, the fact that dimethyl disulfide was detected at the very beginning of the reaction over Mn_2O_3 whereas a period of latency was needed before its appearance over MnO_2. The same observation is also made for the formation of methanol that begins earlier over Mn_2O_3 than over MnO_2.

III.2. Characterizations. *X-ray Diffraction.* The XRD patterns of fresh γ-MnO_2 and samples recovered after 66 h of

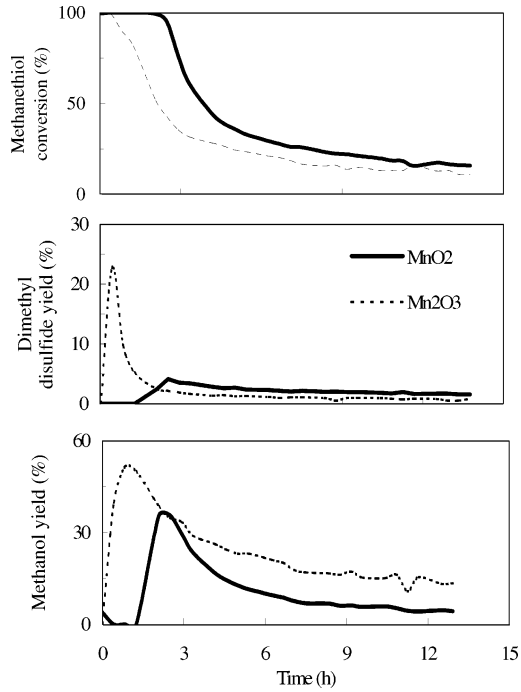

Figure 5. Conversion of 250 vppm of methanethiol and yields of dimethyl disulfide and methanol recorded over 0.1 g of γ-MnO_2 or Mn_2O_3 as a function of the time on stream at 150 °C (total flow 100 mL/min).

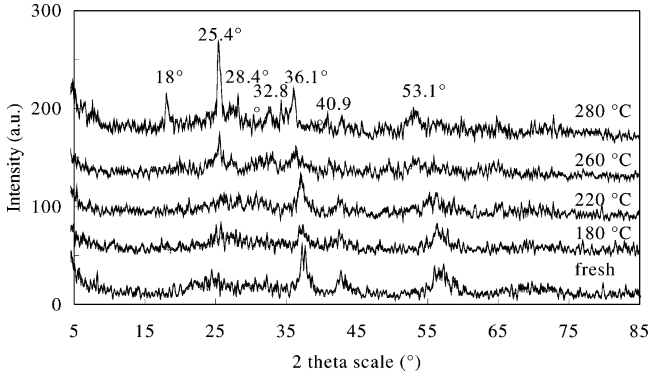

Figure 6. XRD patterns of γ-MnO_2 samples fresh and recovered after 66 h of reaction performed with 250 vppm of methanethiol at 180, 220, 260, or 280 °C.

reaction with 250 vppm of CH_3SH at 180, 220, 260, and 280 °C are presented in Figure 6. At 180 and 220 °C, the diffraction patterns did not present any significant modification with respect to the fresh catalyst: no appearance of a new peak or shift. But at 260 °C and, more intensely, at 280 °C, peaks appeared at 2θ positions of 18.0, 25.4, and 28.4°. These peaks could be attributed to $MnSO_4 \cdot H_2O$ (JCPDS standard file no 33-0906)[27] because they correspond to the position of the most intense peaks of this standard. XRD diffraction analysis has thus clearly evidenced the formation of a manganese sulfate phase whose appearance in diffractograms is dependent on the reaction temperature. However, it must be pointed out that manganese sulfate is very hygroscopic and rapidly transforms into $MnSO_4 \cdot H_2O$.[32] This was experimentally verified on a $MnSO_4 \cdot H_2O$ sample that was calcined at 280 °C for 24 h. Figure 7 clearly shows that although the anhydrous phase was detected over the calcined sample the hydrate phase was also present in this sample, likely resulting from a rehydration proceeding during the transfer and mounting of the calcined sample in the diffractometer. Given that our samples recovered after the test

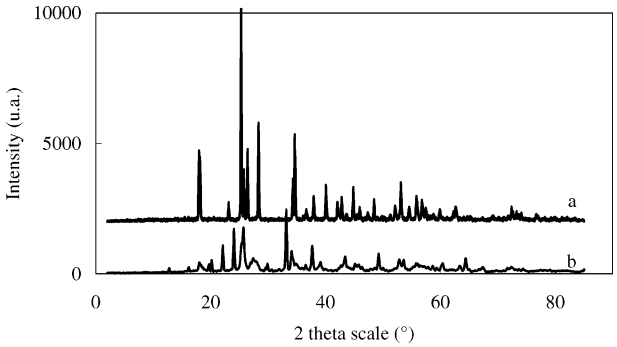

Figure 7. XRD patterns of $MnSO_4 \cdot H_2O$ fresh (a) and after 24 h of calcination at 280 °C (b).

were also handled in air before characterizations, the exact nature of the sulfate phase formed under these reaction conditions (anhydrous vs hydrated) cannot be determined.

However, additional peaks at $2\theta = 32.8$, 36.1, 40.9, and 53.1° detected at 260 and 280 °C did not correspond to any $MnSO_4 \cdot H_2O$ peaks. It should be noted that their low intensity and broad nature made their assignation complicated. According to the electrochemical literature, a reduction of the γ-MnO_2 phase induces a lattice expansion and a shift of its diffraction lines.[33,34] A reduction of γ-MnO_2 may therefore induce a shift of its main broad lines from 37.2, 42.7, and 56° to the peaks detected at 36.1, 40.9, and 53.1°, respectively. Except the peak at 36.1° that could correspond to the main peak of Mn_3O_4 (JCPDS file 24-0734),[27] none of the main peaks of other MnO_x phases could fit the peaks at 36.1 and 40.9°. For example, the main lines of α-Mn_2O_3 are reported at $2\theta = 32.9$ and 55.2° (JCPDS standard file no. 24-0508),[27] but none of its lines could correspond to the 36.1 and 40.9° peaks. Therefore, one cannot fully exclude the occurrence of a small amount of a crystalline phase such as Mn_2O_3, Mn_3O_4, or Mn_5O_8, but no clear evidence proves unequivocally that one of these phases is present. Moreover, no JDPDS standard patterns of manganese sulfates, sulfites, or sulfides fit these peaks. An important reduction of the γ-MnO_2 phase is thus assumed to take place at 260 and 280 °C and results in the shift of the γ-MnO_2 main lines. The 32.8° peak has not yet been assigned. Among all of the JCPDS standard patterns of compounds containing combinations of Mn, O, H, and/or S, this peak could correspond to $MnSO_3 \cdot 2.5H_2O$, $MnSO_4 \cdot 5H_2O$, or $MnSO_4 \cdot 7H_2O$, but because the other main peaks of these standard compounds were less intense or common with $MnSO_4 \cdot H_2O$, an accurate assignment was not possible.

X-ray Photoelectron Spectroscopy. XPS analyses were performed to detect oxidation-state changes and the presence of sulfur on the surface of γ-MnO_2 catalysts after reaction with 250 vppm of methanethiol. The S 2p spectra recorded on the fresh sample and after 15 h of reaction at 150 °C (Figure 8) show that sulfur species clearly appeared on the catalyst surface after reaction with CH_3SH. As shown in Table 1, the identification of sulfur species may be easily achieved because the variation of the sulfur oxidation state induces significant changes in the binding energy of the S $2p_{3/2}$ component. Table 1 summarizes the S $2p_{3/2}$ binding-energy data collected in the literature for various sulfur-containing compounds.

Table 2 presents the S $2p_{3/2}$ binding energies measured on γ-MnO_2 samples recovered after reaction with methanethiol under different conditions (temperatures and durations) and on a commercial $MnSO_4 \cdot H_2O$ sample calcined for 24 h at 280 °C taken as a reference. The 168.3- to 168.8-eV BE values measured after catalytic tests are consistent with sulfur bound to the surface as sulfates in the form of adsorbed species,

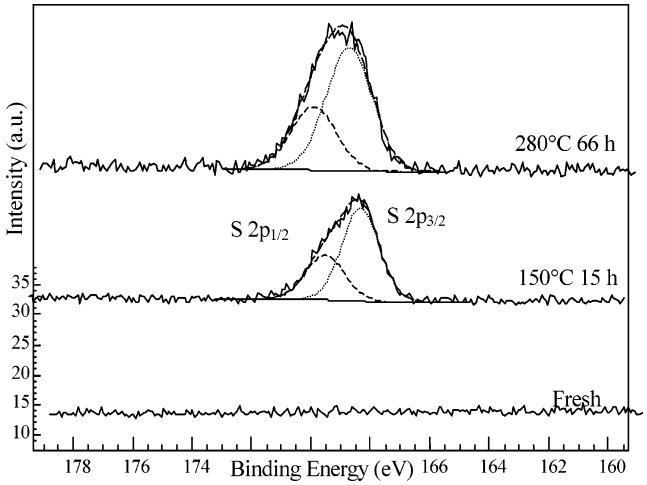

Figure 8. XPS S 2p spectra on γ-MnO_2 before and after reaction with 250 vppm of methanethiol.

TABLE 1: S $2p_{3/2}$ Binding-Energy Attribution of Some Sulfur-Containing Compounds[a]

compound type	S $2p_{3/2}$ binding energy (eV)[b]	refs
elemental sulfur	163.1 − 164.0	31−33
sulfide	160.0 − 163.5	31−35
MnS_2	161.4 − 161.8	34, 35
MnS	161.2	35
sulfite	165.8 − 167.8	31, 33
sulfate	168.0 − 171.5	31−34
$MnSO_4$	168.1, 169.6	33, 34
H_2SO_4 liq/ads	168.4/168.3	36
mercaptan	162.0 − 163.1	31
SO_2	167.0 − 168.2	31
sulfones	166.5 − 170.0	31

[a] From the literature. [b] Corrected binding energy so that the C 1s binding energy corresponds to 284.8 eV.

TABLE 2: XPS Characterizations of γ-MnO_2 after Reaction with 250 vppm CH_3SH at Different Temperatures and after Different Reaction Times[a]

reaction procedure	S $2p_{3/2}$ position (eV)	Δ Mn 3s − satellite (eV)	composition: atomic ratios S/Mn	C/Mn	O/Mn
1. fresh	n.a.	4.9	0	1.29	2.37
2. $MnSO_4 \cdot H_2O$ calcd 280 °C	168.8	6.2	1.33	1.55	5.45
3. MSH, 150 °C, 3 h	168.4	4.9	0.16	0.53	2.50
4. MSH, 150 °C, 15 h	168.3	5.0	0.24	0.58	2.76
5. MSH, 180 °C, 15 h	168.4	5.0	0.18	0.76	2.66
6. MSH, 180 °C, 66 h	168.3	5.0	0.28	0.84	3.02
7. MSH, 220 °C, 15 h	168.4	5.2	0.21	0.86	2.78
8. MSH, 220 °C, 66 h	168.7	5.4	0.53	0.98	3.67
9. MSH, 260 °C, 66 h	168.8	5.8	0.81	0.88	4.12
10. MSH, 280 °C, 66 h	168.8	5.8	0.38	0.53	2.50

[a] Sample 2, commercial $MnSO_4 \cdot H_2O$ calcined at 280 °C, serves as a reference.

$MnSO_4$, or possibly sulfones. A comparison of the C 1s spectra of the catalysts before and after reaction did not evidence any shape modification. The carbon species detected on the surface by XPS mainly arose from the usual contaminant carbon. C 1s peaks could generally be decomposed into three components. The main component is given by the *C*−C,H species (284.8 eV), and the two smaller ones come from *C*−O species (around 286.3 eV) and O−*C*=O species (around 288.5 eV). Because the binding energy of carbon bound to sulfur is the same as for *C*−O species[35] and because the C 1s peak shapes did not change after reaction, the possible presence of sulfur-containing organic compounds, especially sulfones, should be negligible compared to the presence of sulfate species. However, a modification of the sulfate state was noticed because the S $2p_{3/2}$ peak position was shifted from 168.3 to 168.8 eV with increasing temperature. Dijs et al.[40] have observed a higher binding energy of S $2p_{3/2}$ for bulk $Zr(SO_4)_2$ (170 eV) than for adsorbed sulfuric acid on zirconium hydroxide (168.3 eV). The 168.8-eV position corresponds well to the value measured on the manganese sulfate sample, whereas the lower BE position around 168.3 eV would be better assigned to adsorbed "sulfuric acid-like" species.

The oxidation state of manganese may be accurately evaluated by means of the distance between the Mn 3s peak and its satellite.[41,42] A reduction of the manganese oxidation state induces an increase in the distance between Mn 3s bands.[42] The values of Mn 3s splitting (i.e., the differences in binding energy between Mn 3s and its satellite) are reported in Table 2. These results show that an important surface reduction of the samples occurs after reaction at 260 and 280 °C. Samples after reaction at 220 °C exhibit an intermediate reduction state. At lower temperature, the surface reduction occurring on γ-MnO_2 in the presence of methanethiol is weak and does not exceed the normal reduction state encountered by γ-MnO_2 during the oxidation of VOCs that do not contain sulfur.[43,44]

Table 2 also summarizes the S/Mn, C/Mn, and O/Mn atomic ratios. An increase in sulfur content was observed with increasing time on stream at a given temperature and with increasing temperature up to 260 °C. However, a decrease in the S/Mn ratio was found on the catalyst characterized after reaction at 280 °C. This diminishing of the S/Mn ratio after reaction at 280 °C was checked on an additional sample.

Concerning the C/Mn ratio, a decrease in carbon content was observed after reaction, although an increase in carbon content due to the adsorption of organic compounds on the surface might have been expected. This further confirms the idea that if sulfur-containing organic compounds are adsorbed on the catalyst surface they are present in very small quantities.

The O/Mn ratio increased after reaction with methanethiol and followed the sulfur accumulation. In addition to an increase in the O/Mn ratio, the O 1s peak also underwent a dramatic shape modification with reaction. Its evolution with reaction temperature and time on stream is illustrated in Figures 9 and 10, respectively. On the fresh γ-MnO_2 sample, the fitting of the asymmetrical oxygen peak may be performed with two components. The main component at lower BE (529.5 eV) is attributed to the oxygen of the manganese oxide lattice.[35,45] The assignment of the second highest BE (531.5 eV) component is more complex because of the combination of different oxygen species arising from OH groups, H_2O, the contaminant organic matrix, and so forth.[35,45] After reaction with methanethiol, an increase in the intensity of the higher-binding-energy component of the O 1s peak was observed for all samples (Figures 9 and 10). As the reaction temperature or the time under the reactant flow increased, the contribution of this higher-BE component to the O 1s peak shape progressively grew and became superior to the lower BE component. As measured on the commercial manganese sulfate sample, the O 1s binding energy for a sulfate group is centered around 531.7 eV. Thus, the observed increase in the higher-binding-energy component (O_{surf}/Mn ratio in Table 3) agrees with the augmentation of oxygen due to the accumulation of sulfate species. Indeed, Figure 11 shows that a linear relationship was obtained between the sulfur content (S/Mn ratio as reported in Table 2) and the O 1s higher-binding-energy component (O_{surf}/Mn ratio given in Table 3). This relation

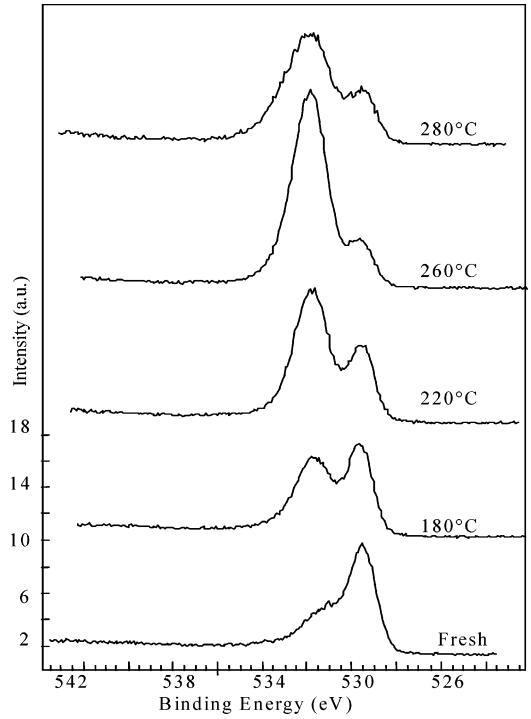

Figure 9. Evolution of the O 1s XPS peak of γ-MnO_2 with the reaction temperature after 66 h of reaction under 250 vppm of methanethiol.

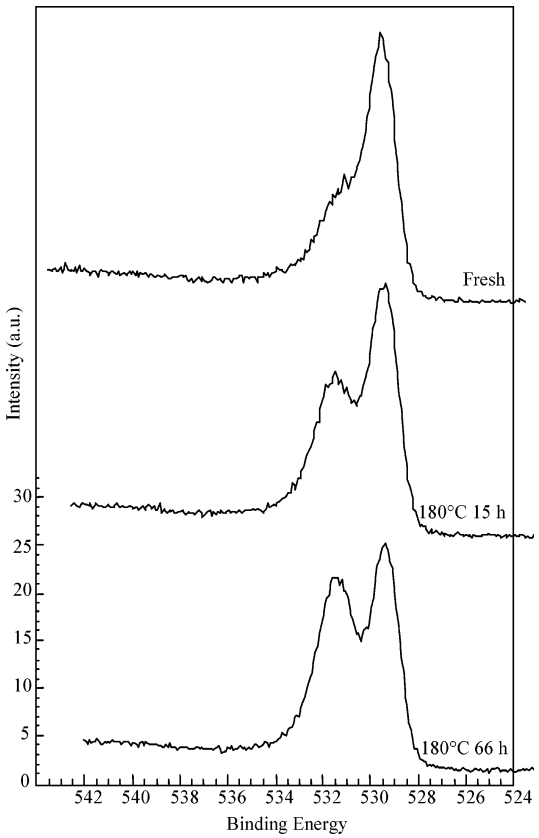

Figure 10. Evolution of XPS O 1s of γ-MnO_2 with the time on stream of the reaction under 250 vppm of methanethiol at 180 °C.

confirms that the growth of the O_{1s} higher-binding-energy component may mainly be attributed to the increase of the sulfate species on the surface. All of the data collected on γ-MnO_2 samples recovered after testing with 250 vppm methanethiol at temperatures varying from 150 to 280 °C are included in the plot reported in Figure 11. However, it is clearly shown

TABLE 3: O 1s Peak Decomposition Results and Contributions of the Different Oxygen Species to the Higher-Binding-Energy Component

	composition, atomic ratio				
	decomposition of O 1s peak		O−S/		
reaction procedure	O_{lat}/Mn (~529.5 eV)	O_{surf}/Mn (~531.5 eV)	Mn as SO_4^{2-} [a]	O−C/ Mn[b]	O−H/ Mn[c]
1. fresh	1.27	1.10	0.00	0.60	0.51
2. MSH, 150 °C, 3 h	1.26	1.24	0.64	0.19	0.41
3. MSH, 150 °C, 15 h	1.27	1.50	0.97	0.18	0.35
4. MSH, 180 °C, 15 h	1.32	1.34	0.72	0.32	0.30
5. MSH, 180 °C, 66 h	1.28	1.74	1.11	0.35	0.28
6. MSH, 220 °C, 15 h	1.23	1.55	0.85	0.43	0.26
7. MSH, 220 °C, 66 h	1.05	2.62	2.12	0.38	0.12
8. MSH, 260 °C, 66 h	0.60	3.51	3.24	0.36	−0.08
9. MSH, 280 °C, 66 h	0.55	2.74	1.52	0.43	0.79

[a] Calculated from the value of S/Mn in Table 2 multiplied by 4. [b] Calculated from the sum of the C 1s component at 286.3 eV plus twice the component at 288.5 eV. [c] Calculated from the subtraction of O in SO_4^{2-} and O−C, with O = C contributions from the O_{surf}/Mn component.

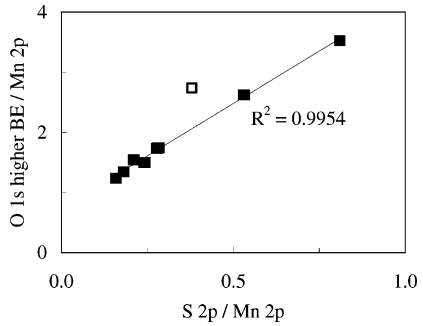

Figure 11. Relationship between the S 2p/Mn 2p ratio (values reported in Table 2) and O 1s higher-BE component/Mn 2p ratio (values reported in Table 3). All data measured after the test under different conditions of temperature from 150 to 280 °C over γ-MnO_2 are included in this graph. The point marked with □ corresponds to the catalyst after 66 h of reaction at 280 °C.

that the sample characterized after reaction at 280 °C largely deviated from this linear relationship. This deviation of the sample after reaction at 280 °C was checked on another sample. A diminishing of the sulfur content measured by XPS has previously been observed between 260 and 280 °C (Table 2). These observations seem to indicate that modifications of the catalyst surface occur between 260 and 280 °C, affecting sulfur and oxygen compositions in a different way. As observed in Figure 11, the oxygen contribution of the sample after reaction at 280 °C appeared superior to that expected on the basis of the XPS sulfur content. In addition to oxygen in sulfate species, the presence of oxygen bound to carbon or hydrogen may contribute to the higher-binding-energy component of the O 1s peak. As already mentioned, the decomposition of the O 1s peaks is complex because of the simultaneous presence of oxygen bound to carbon, hydrogen, and sulfur in the same binding-energy region. Nevertheless, Table 3 presents an attempt to calculate the contribution of the different O 1s species. As reported in the literature for sulfated zirconia samples,[46,47] the oxygen peak was decomposed into two components. The low-binding-energy component centered around 529.5 eV (defined as O_{lat} in Table 3) was assigned to the lattice oxygen of the oxide. The higher-binding-energy component located around 531.6 eV (defined as O_{surf} in Table 3) included the whole set of oxygen species bound to sulfur, hydrogen, and carbon. The sulfate oxygen contribution was calculated from the sulfur content multiplied by 4, assuming that all of the sulfur was

present as the SO_4^{2-} species. The contribution of the oxygen linked to carbon was evaluated using the decomposition of the C 1s peak: the sum of the component at 286.3 eV belonging to C−O species plus 2 times the component at 288.5 eV for O−C═O species. The oxygen bound to hydrogen belonging to surface hydroxyls and the water of hydration was finally calculated from the subtraction of the two previous contributions from the O 1s highest-BE component. Because the O_{lat} component was attributed to the amount of oxygen bound to manganese, its ratio to Mn should represent the stoichiometric ratio of oxygen in manganese oxide. However, the O_{lat}/Mn ratio of the fresh γ-MnO_2 was equal to 1.3 and thus differed largely from the stoichiometric value of two oxygen atoms per manganese atom. The presence of superficial hydroxyl groups and surface defects should decrease the surface O/Mn composition of oxide compared to the bulk composition. Besides, ratios are affected by the decomposition parameters and sensitivity factors. In this work, different decompositions and quantifications of the set of data have been performed using two different programs of decomposition. We found that the experimental choice of the baseline shape, decomposition parameters, and so forth influenced the absolute values of the ratios but did not affect the general tendency observed between the different samples. The aim of this part is therefore not to interpret the discrete value of the ratios calculated in Table 3 but rather to study their evolution with the time and temperature of reaction. The value of the O_{lat}/Mn ratio remained constant for samples characterized before and after reaction at 150 or 180 °C, but after reaction at 220 °C, the ratio began to decrease. When reaction temperatures reached 260 and 280 °C, the O_{lat}/Mn ratio strongly decreased even further. The decreases in the amount of O bound to manganese indicate that a reduction of the manganese state is occurring. These observations are in very good agreement with the information deduced from the observed decrease of the Mn 3s band splitting with increasing temperature. The O−C/Mn contribution (reported in Table 3) arose from a carbonaceous organic contaminant deposited on the catalyst surface and varied in parallel to the C/Mn ratio reported in Table 2. However, the O−H/Mn ratio decreased progressively with the reaction time and with the reaction temperature up to 260 °C. The decrease may be attributed to the disappearance of hydroxyl groups or structural water from the catalyst surface. Nevertheless, a sharp increase in O−H/Mn was observed for samples reacting at 280 °C. In addition to this increase in the O−H contribution, a decrease in the S−Mn ratio and a deviation from the linear relationship observed in Figure 11 (plot between the S/Mn and O 1s higher-BE component) was also reported for this sample recovered after reaction at 280 °C. To explain these observations, we can state that the modification of surface composition encountered by samples recovered after reaction at 280 °C is due to a deeper crystallization of the hydrated manganese sulfate phase. This transformation should induce a higher incorporation of sulfur into the bulk catalyst (decreasing the surface S/Mn ratio) and an increase in the water-of-hydration content (increasing the O−H/Mn ratio). The formation of a $MnSO_4 \cdot H_2O$ phase by XRD over γ-MnO_2 samples was indeed most clearly evidenced after reaction at 280 °C. However, we have also underlined the fact that the anhydrous phase tends to be rapidly hydrated. Because samples were manipulated in air before analysis, we cannot determine whether O−H groups exist at the catalyst surface during the reaction or come from ex situ hydration.

In summary, XPS results clearly indicate that sulfate species are present on the catalyst surface after reaction with methanethiol, whatever the temperature. The amount of sulfate deposited on the surface increases with the reaction time at a given temperature and with the reaction temperature. In addition to sulfation, the γ-MnO_2 catalyst underwent a reduction. The reduction of the catalyst was very low at low temperatures (150 and 180 °C), but it was important after reaction at 260 and 280 °C. Moreover, a change in the binding energy of the S $2p_{3/2}$ component is also noticed between these two domains of temperature. At high temperatures (260 and 280 °C), the position of S $2p_{3/2}$ corresponds well to that measured on commercial manganese sulfate, whereas it is better assigned to adsorbed sulfuric acid-like species at the lower temperatures (150 and 180 °C).

TABLE 4: Potentiometric Evaluation of the Average Oxidation State of Manganese in γ-MnO_2 Samples after Reaction with 250 vppm of Methanethiol (MSH) under Different Conditions

reaction procedure	potentiometric evaluation of the average Mn oxidation state
1. fresh γ-MnO_2	3.9
2. MSH, 150 °C, 1 h 30	3.7
3. MSH, 150 °C, 3 h	3.7
4. MSH, 150 °C, 15 h	3.7
5. MSH, 180 °C, 15 h	3.7
6. MSH, 180 °C, 66 h	*a*
7. MSH, 220 °C, 15 h	3.5
8. MSH, 220 °C, 66 h	3.5
9. MSH, 260 °C, 66 h	*a*
10. MSH, 280 °C, 66 h	3.0

[a] Not measured.

Potentiometric Determination of the Manganese Oxidation State. The determination of Mn^{4+} and total manganese concentrations by potentiometric titration analysis allows us to evaluate the average oxidation state of bulk manganese. The average oxidation states of manganese in samples before and after reaction are presented in Table 4. After reaction with methanethiol, a reduction of the catalyst samples occurred. As the reaction temperature increased, the degree of reduction increased. As observed at 150 °C, the reduction of the catalyst occurred very rapidly because it had already been detected after 1.5 h of reaction when 100% MSH conversion was recorded. The degree of reduction reached by the catalyst at this time was then kept stable for at least 15 h at 150 and 180 °C. Higher reduction states of manganese were measured after reaction at 220 °C and in an even more pronounced way at 280 °C.

Ex Situ DRIFTS Study of the Catalysts after Reaction with Methanethiol. DRIFTS spectra of some samples were recorded on used catalysts recovered after catalytic tests. All spectra were obtained at room temperature in the ambient atmosphere without any heating or flushing. Figure 12 shows the spectra of fresh and used γ-MnO_2 samples. The spectrum of fresh γ-MnO_2 shows a large band around 760 cm^{-1} that may be assigned to the Mn−O vibrational mode in the MnO_2 lattice.[48] All spectra of fresh and used MnO_2 present a very broad band centered at about 3400 cm^{-1} due to unresolved ν(OH) vibrations of surface hydroxyl groups and coordinated and physisorbed water. These bands were accompanied by the poorly resolved bands around 1640 cm^{-1} due to δ(O−H) vibrations. After reaction with methanethiol at 150 °C for 15 h, a strong band around 1230 cm^{-1} and two weak bands at 1338 and 1064 cm^{-1} appeared in the spectra. After 66 h at 180 °C, no shift in band intensity and no change in band ratio intensity were noticed with respect to the spectra recorded for the 150 °C sample (curve b). However,

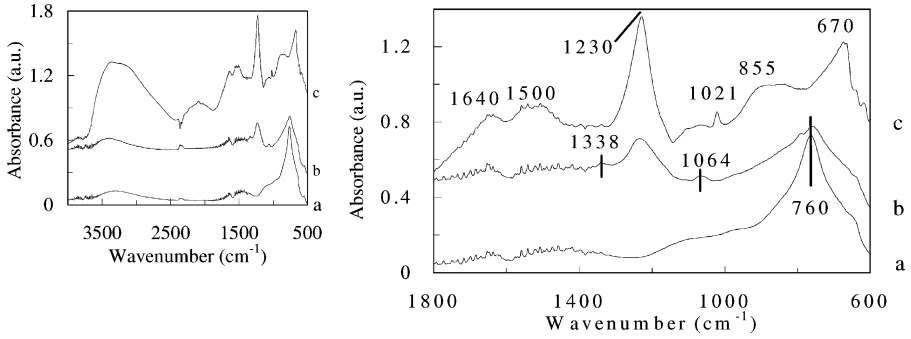

Figure 12. DRIFTS spectra recorded at room temperature in ambient air of fresh γ-MnO_2 (a) and of samples recovered after the test with 250 vppm of methanethiol at 150 °C (b) and 280 °C (c).

important changes were observed in the spectrum of MnO_2 recovered after reaction at 280 °C. The lattice band was noticeably shifted toward a lower wavenumber around 670 cm^{-1} and presented a shoulder around 855 cm^{-1}. Furthermore, the bands at ~1230 cm^{-1} and the broad band in the OH region were largely increased compared to those for 150 °C. The weak band at 1338 cm^{-1} was not detected anymore and the one at 1064 cm^{-1} had almost fully disappeared, whereas a small band at 1021 cm^{-1} and broad bands around the 1500- and 2100-cm^{-1} regions appeared in the spectrum. Clear assignments of these bands were not an easy task because various species could be formed and stayed adsorbed on the catalyst surface in addition to the structural modification of the catalyst. However, previous characterizations have shown the presence of a significant amount of sulfur principally in the form of sulfate species.

Because the adsorption of methanethiol is the first phenomenon that was likely to take place on the catalyst surface, the infrared bands of adsorbed methanethiol were considered first. According to Bensitel et al.,[49] the adsorption of CH_3SH gives rise to strong bands in the 3000−2800-cm^{-1} (due to C−H vibrations) and 2500−2600-cm^{-1} (due to ν(S−H)) regions. In our spectra, the presence of CH_x and SH species was not found. As mentioned above for XPS analysis, the presence of adsorbed organic compounds could not be excluded, but their amount on the catalyst surface should be very low. The band positions of sulfate species collected in the literature were then compared to our spectra. According to the literature, the bands above 1300 cm^{-1} may be assigned to the ν(S═O) vibrational mode of sulfate species, whereas those below 1100 cm^{-1} correspond to the ν(S−O) vibrations.[50−52] The spectrum of a sulfated Mn_2O_3 sample has been recorded by Kijlstra et al.[9] after pretreatment in vacuum at 150 °C. This spectrum was characterized by a broad band around 1180 cm^{-1} characteristic of bulk $MnSO_4$ and a smaller band at 1350 cm^{-1} assigned to the $\nu(S{=}O)_{as}$ of surface manganese sulfate. The band at 1338 cm^{-1} recorded at 150 and 180 °C is thus attributed to the presence of sulfate on the manganese surface, and the band at 1064 cm^{-1} could correspond to ν(S−O) vibrations of sulfate. No band around 1180 cm^{-1} was observed on our spectra, though a bulk manganese sulfate phase was detected by XRD at 280 °C. In contrast, an intense band around 1230 cm^{-1} was found in the spectra of all used catalysts. Although the position of this band was outside the usual region reported for sulfate species (see above), the work of Babou et al.[52] has shown that the hydration of sulfated samples can cause important shifts of sulfate IR bands. In their work, they have reported the IR bands of adsorbed H_2SO_4 and have attributed a band around 1250 cm^{-1} to the $\nu(S{=}O)_s$ of adsorbed H_2SO_4. Moreno and Poncelet[54] have also reported band shifts due to hydration and have noticed the recovery of a band at ~1250 cm^{-1} when partial rehydration of their sulfated samples occurred. The observation of sulfate bands

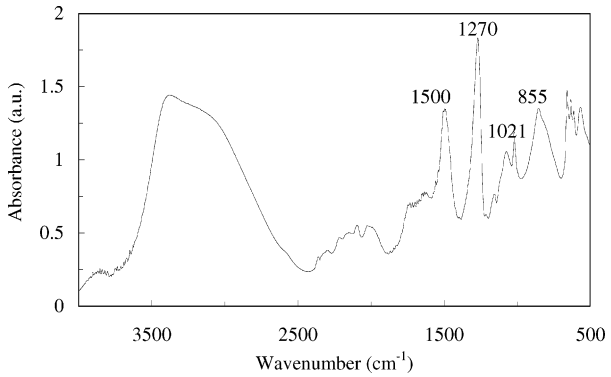

Figure 13. DRIFTS spectra of $MnSO_4{\cdot}H_2O$ recorded at room temperature in ambient air.

in the 1200−1300-cm^{-1} region thus appeared to be associated with the hydration of the surface, and the band around 1230 cm^{-1} may be attributed to hydrated sulfate species. To confirm this assignment, the DRIFTS spectrum of $MnSO_4{\cdot}H_2O$ has been recorded and is shown in Figure 13. In addition to a very broad band in the OH stretching region around 3400 cm^{-1}, many bands below 2500 cm^{-1} characterize the $MnSO_4{\cdot}H_2O$ sample. Our measurements clearly show that an intense band was observed around 1270 cm^{-1} in the hydrated sulfate region. Moreover, no intense band around 1180 cm^{-1} corresponding to anhydrous manganese sulfate is observed in this spectrum. Large bands were also found around 1500 and 855 cm^{-1}. According to Ohnishi et al.,[55] the band around 855 cm^{-1} is characteristic of the rocking mode of the water of crystallization of $MnSO_4{\cdot}H_2O$. The sharp bands below 660 cm^{-1} are most likely due to Mn−O vibrations. The spectrum of MnO_2 recorded after reaction at 280 °C showed many bands and was similar to the spectrum of $MnSO_4{\cdot}H_2O$. After reaction at 280 °C, a $MnSO_4{\cdot}H_2O$ phase was also detected by XRD. As indicated by the Mn−O vibration shift and the bands at about 1021, 2100, and 855 cm^{-1} as in the $MnSO_4{\cdot}H_2O$ spectrum, a phase transformation occurred during the reaction at 280 °C that also induced important modifications in the infrared spectrum. These results thus confirm the transformation of MnO_2 into a manganese sulfate phase at 280 °C. In contrast, no significant structural modification of MnO_2 affecting the manganese lattice took place at 150 and 180 °C, although some sulfate species are detected. Interpretations of the spectra collected in this work were rather complicated because most infrared studies found in the literature are made after outgassing, causing the dehydration of samples and subsequent band shifts. In our opinion, this work reported for the first time the true band position for a hydrated manganese sulfate sample. The aim of our work was to identify as far as possible the species that were formed under our reaction conditions. However, samples were handled and analyzed in

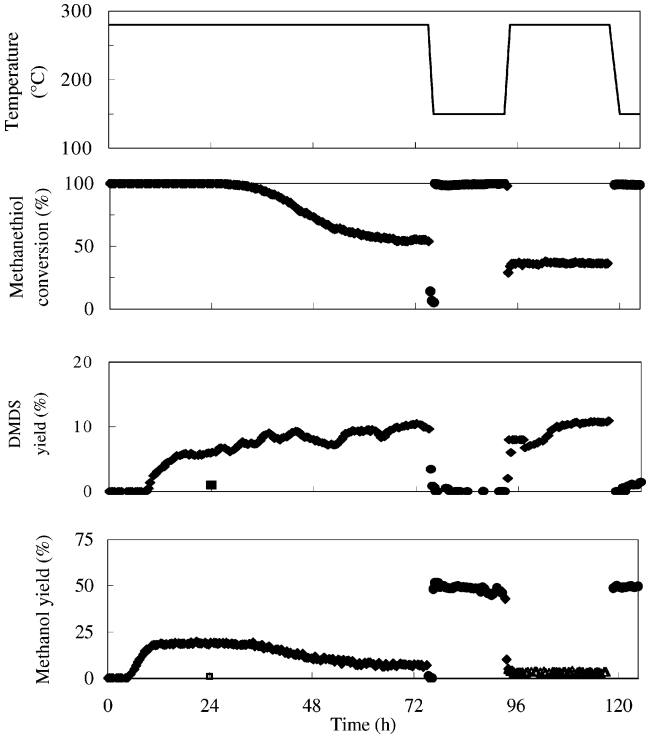

Figure 14. Conversion of 250 vppm of methanethiol, yields of dimethyl disulfide and methanol recorded over γ-MnO_2 as a function of the time on stream and reaction-temperature variations (from 280 to 150 then 280 and back to 150 °C).

ambient air. As reported for XRD and XPS, anhydrous $MnSO_4$ easily adsorbs water and transforms into $MnSO_4 \cdot H_2O$.

III.3. Evolution of the γ-MnO_2 Activity with Cyclic Variations of the Reaction Temperature. Figure 14 presents the evolution of the activity of the γ-MnO_2 catalyst with the time on stream and successive variations of the temperature between 280 and 150 °C. The test was initially performed at 280 °C to reach a stable conversion of methanethiol (after ~3 days). The temperature was then decreased to 150 °C. The decrease in temperature was first accompanied by a decrease in the methanethiol conversion to less than 20%, but after a period of about 1 h, the conversion of methanethiol suddenly grew to 100%. In the same time, the yield of methanol increased up to 50%, but dimethyl disulfide was no longer produced. The temperature of the test was then again increased up to 280 °C. The conversion of methanethiol and the yield of methanol were diminished, and the yield of dimethyl disulfide increased. A decrease in the temperature to 150 °C once more caused an increase in the conversion of the methanethiol and the yield of methanol as well as a decrease in the formation of dimethyl disulfide.

A test was also performed first by deactivating a fresh γ-MnO_2 sample at 150 °C for 15 h. Figure 15 shows that although the catalyst is strongly deactivated at 150 °C an increase in the temperature to 280 °C for 24 h allows us to reactivate the catalyst, which then becomes active after the temperature decreases to 150 °C.

IV. Discussion

IV.1. Evolution of Sulfate Species and the Reduction State with the Reaction Temperature. Although XPS and DRIFTS evidenced the presence of sulfur species at the catalyst surface, samples characterized after reaction at 150 and 180 °C exhibited no modification of their XRD diffraction patterns. On these

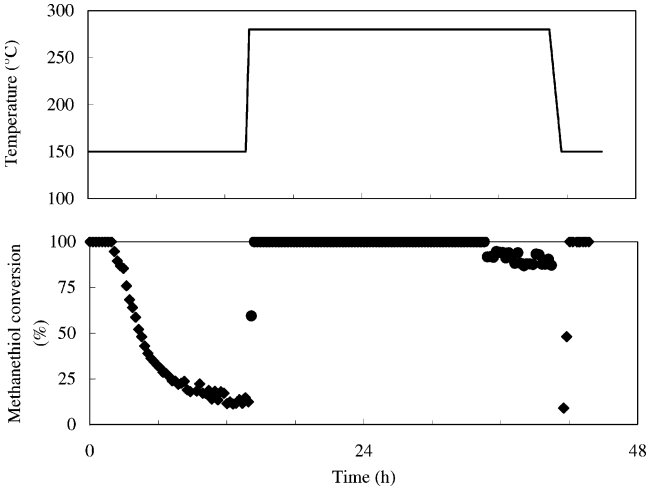

Figure 15. Conversion of 250 vppm of methanethiol, yields of dimethyl disulfide and methanol recorded over γ-MnO_2 as a function of the time on stream and reaction-temperature variations (from 150 to 280 and back to 150 °C).

samples, the position of the S 2p3/2 peak was centered around 168.4 eV and was inferior to the binding energy of the reference manganese sulfate sample (168.8 eV) but can nonetheless be assigned to adsorbed sulfate species (most likely in the form of adsorbed sulfuric acid-like species).[40] The new band centered around 1230 cm^{-1} observed in the DRIFTS spectrum after reaction at 150 °C was also assigned to hydrated sulfate species. Furthermore, a slight reduction of the manganese oxidation state was evidenced by XPS and potentiometric analysis on the same samples. An equivalent degree of reduction of the γ-MnO_2 catalyst was found to occur during the oxidation of non-sulfur-containing VOCs such as *n*-hexane and trimethylamine.[43,44] Moreover, potentiometric analysis indicated that this reduction of the catalyst rapidly took place and has already reached a stable value after 1.5 h of reaction (i.e., when the MSH conversion was still complete). Although no further reduction of the catalyst was observed upon increasing the time on stream, the amount of adsorbed sulfate species on the surface kept increasing as the reaction proceeded. The appearance of a bulk manganese sulfate phase was observed only by XRD when reactions were performed at higher temperatures (i.e., 260 and 280 °C). Moreover, the XPS analysis of these samples showed a shift of the S 2p3/2 peak from 168.4 to 168.8 eV, accompanied by a deep reduction of manganese, as confirmed by the large increase in the Mn 3s band splitting. The important reduction of the bulk manganese oxidation state above 260 °C was also indicated by the potentiometric measurements. Moreover, DRIFTS analysis of the sample reacted at 280 °C showed important structural modifications, as shown by the shift in the region of the Mn−O vibrations.

These results led us to define two regions of temperature that are assumed to correspond to the formation of different types of sulfate species:

− A low-temperature region below 200 °C where the sulfate species accumulated on the γ-MnO_2 catalyst surface in the form of adsorbed sulfate species and most likely adsorbed sulfuric acid-like species. The formation of a bulk sulfate phase in this region may be limited by the weak reduction encountered by the γ-MnO_2 catalyst and the fact that Mn(III) and Mn(IV) species do not form stable sulfates.[22,56]

− A higher-temperature region where the diffusion of the sulfate species into the bulk and the reaction with manganese species resulted in the formation of a new manganese sulfate

phase ($MnSO_4$ or $MnSO_4 \cdot H_2O$). This region was also characterized by an important reduction of the manganese dioxide phase. The deeper reduction of the manganese ions observed in this higher-temperature region could induce the formation of the stable manganese(II) sulfate phase. On the contrary, the higher temperature could also favor the reaction of sulfate species with manganese ions and cause their reduction and the formation of the stable manganese(II) sulfate phase. It is, however, difficult to determine if it is the reduction that is responsible for the sulfation or the contrary.

The formation of different types of sulfate species as a function of temperature was suggested by Otsuka et al.[24,25] during the direct reaction of MnO_2 with SO_2. Their infrared and activity results suggested the presence of adsorbed sulfate groups on the first layers of the catalyst surface at temperatures below 200 °C, whereas bulk manganese sulfate was formed at higher temperatures. Moreover, our XPS and DRIFTS experiments seem to indicate that the adsorbed sulfate species are most likely in the form of adsorbed sulfuric acid-like species. This assignment is in agreement with the observation of Sultanov et al.,[17] who stated that the first step in the deactivation of oxide catalysts was the conversion of SO_3 to H_2SO_4, which then can react with the solid to form metal sulfates.

IV.2. How Does the Formation of These Sulfate Species Influence the Catalytic Activity? For non-sulfur-containing volatile organic compounds, the reactions of total oxidation over the γ-MnO_2 catalyst proceed at least partially through a Mars and van Krevelen type of mechanism.[43] According to this mechanism, the oxidation of adsorbed molecules proceeds through the participation of the lattice oxygen of the oxide. The regeneration of the used sites occurs via reoxidation by the oxygen coming from the gaseous feed.[57] We have shown that the occurrence of this mechanism over a γ-MnO_2 catalyst provokes a slight reduction of the catalyst (because of an insufficient reoxidation step).[43] After a period of 1.5 h at 150 °C, reaction with methanethiol also induced a slight reduction of the catalyst bulk and surface, which is equivalent to the reduction detected after reaction with non-sulfur-containing VOCs.[43,44] In the low-temperature region (below 200 °C), the manganese reduction state appears to be maintained with the time on stream at the stable value of 3.7. As for non-sulfur-containing VOCs, this rapid and stable reduction may be explained by the participation of the lattice oxygen of the catalyst in the oxidation of the methanethiol molecule. At the beginning of the reaction, the oxidation of S−VOCs seems to follow the Mars and van Krevelen mechanism, as observed for other volatile organic compounds. However, a decrease in the conversion efficiency was observed with the time on stream. The rate of this decrease was nonetheless dependent on the reaction temperature. Figure 4 shows that *n*-hexane conversion was quickly inhibited by the presence of methanethiol whereas the methanethiol conversion remained unaffected. The fast inhibition of VOC conversion by another VOC has been formerly explained by the competition of VOC adsorption sites.[43,44] The experiment with *n*-hexane and methanethiol showed that methanethiol adsorption takes place at the beginning of the reaction and inhibits *n*-hexane adsorption. Nevertheless, no significant accumulation of organic compounds was identified by XPS and DRIFTS, but increasing amounts of sulfate species were detected. The results therefore suggested that the methanethiol molecules are progressively oxidized by the catalyst through the Mars and van Krevelen mechanism and initiate the formation of sulfate compounds that modify the catalyst activity. Because different kinds of sulfate species are formed according to the temperature (i.e., adsorbed sulfate species (sulfuric acid-like species) or manganese sulfate phase), different processes of deactivation are also assumed to occur in the two temperature regions.

In the low-temperature region (below 200°C), we have shown that a progressive accumulation of sulfate species occurred at the surface of the catalyst. A continuous increase of the reduction should imply that the reoxidation of the catalyst by molecular oxygen would be inhibited. Because no further catalyst reduction accompanied the decrease in activity, the adsorbed sulfate species progressively formed during the reaction are assumed to poison the methanethiol adsorption sites and therefore their oxidation through the Mars−van Krevelen mechanism. A mechanism of sulfur poisoning based on the blockage of adsorption sites by adsorbed SO_x species was proposed for various catalysts by Liao et al.,[58] Farrauto and Wedding,[59] and Oudar.[14]

In the high-temperature region (260−280°C), the conversion of methanethiol must be enhanced by the improved oxygen mobility of the catalyst. As a consequence, the reduction of the catalyst and sulfate formation should also increase. Moreover, the higher temperature must favor the diffusion of surface sulfate species into the bulk and their reaction with reduced manganese ions to form a new manganese sulfate phase. After 66 h at 260 or 280 °C, the coexistence of two main phases has been detected by XRD: a reduced manganese oxide and a manganese sulfate phase. Heyes et al.[16] have reported that a sulfated MnO_2 catalyst remains moderately active in the oxidation of VOCs. Moreover, they also showed that a manganese sulfate sample is active in the conversion of methanethiol.[19] However, they observed an important decrease in activity between 200 and 300 °C that they could not explain. Recently, we have shown that manganese sulfate is actually a very active catalyst in this reaction but below 240 °C when it is maintained in its hydrated $MnSO_4 \cdot H_2O$ form.[20] Indeed, the loss of the hydration water provokes a high decrease in the activity of the manganese sulfate. We have also shown that the hydration/dehydration of the manganese sulfate phase and subsequent activation/deactivation are a reversible phenomena.[20] The present work shows that the formation of the bulk manganese sulfate phase identified after the reaction of γ-MnO_2 at 280 °C presents an activity and a behavior similar to those of the commercial $MnSO_4 \cdot H_2O$ sample. Moreover, the decrease in temperature to 150 °C was accompanied by an increase in the yield of methanol and the disappearance of DMDS formation in the same way as previously observed with the commercial $MnSO_4 \cdot H_2O$ sample. However, Figure 14 shows that a high activity at 150 °C is induced after the catalyst has reacted with 250 vppm of methanethiol at 280 °C. Moreover, a γ-MnO_2 catalyst, which was deactivated at 150 °C, can become highly active at this temperature only after going up to 280 °C for a few hours (Figure 15). This experiment clearly confirms the formation of different types of sulfate species (adsorbed vs bulk) in the two temperature regions. Because very low activities and deep deactivation were recorded over γ-MnO_2 for reactions performed at 150 and 180 °C, an active manganese sulfate phase is not formed in this low-temperature region. Higher temperatures are indeed necessary to achieve the reaction of the adsorbed sulfate species with manganese ions to form the bulk manganese sulfate phase. Although the $MnSO_4 \cdot H_2O$ phase was detected over γ-MnO_2 after reaction at 280 °C, we have already explained that samples were handled in air before characterizations and that the anhydrous manganese sulfate phase is very hygroscopic. This explains why the monohydrate phase was detected over samples after reaction at 280 °C. The activation of the catalyst

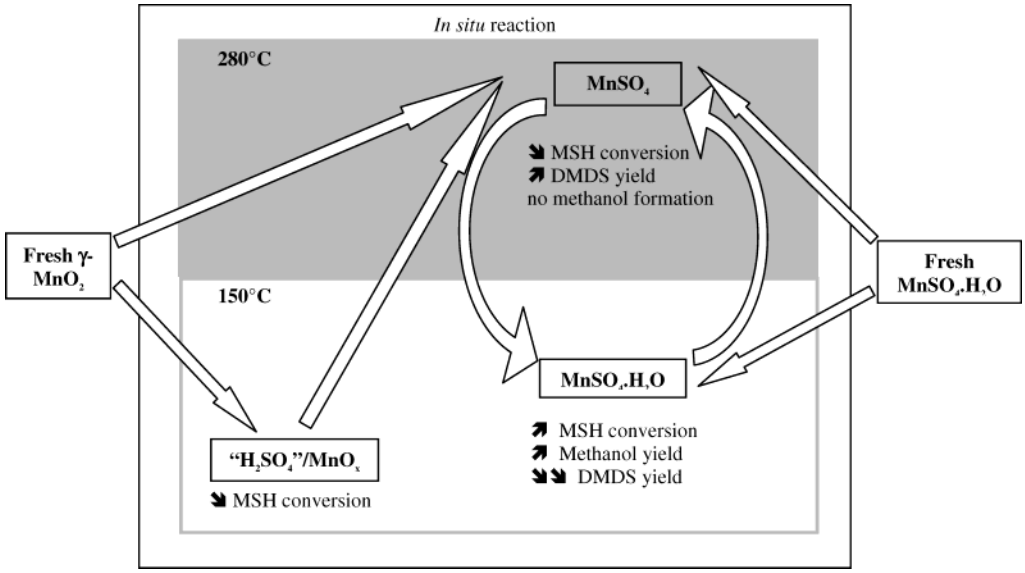

Figure 16. Schematic representation of the catalyst modifications of γ-MnO_2 and $MnSO_4 \cdot H_2O$ during their reaction with methanethiol.

observed with the decreases in temperature from 280 to 150 °C can be related to the hydration of the manganese sulfate phase with the water produced by the oxidation of methanethiol. These results indicate that the manganese sulfate phase formed by the reaction of sulfate species with γ-MnO_2 in the higher-temperature region is very likely in its anhydrous form. The behaviors of the γ-MnO_2 and $MnSO_4 \cdot H_2O$ catalysts during their reaction with methanethiol and the changes they undergo with variations in temperature are schematically summarized in Figure 16.

IV.3. Influence of Catalyst Modifications on the Formation of the Two Main Organic Products: Methanol and Dimethyl Disulfide. Dimethyl disulfide and methanol were identified as the two main products of methanethiol incomplete oxidation over γ-MnO_2, Mn_2O_3, and $MnSO_4 \cdot H_2O$. According to the work of Dalai et al.,[28] dimethyl disulfide is formed according to this oxidation reaction: $2CH_3SH + {}^1/_2O_2 \rightarrow (CH_3)_2S_2 + H_2O$ (1). This reaction involves the interaction of two CH_3S- species arising from S−H bond scission in CH_3SH. However, the formation of methanol results from the rupture of the C−S bond, giving rise to CH_3- species.[29] Different kinds of organic species must therefore be present on the catalytic surface during the oxidation of methanethiol. Nevertheless, dimethyl sulfide (DMS) was never detected. Moreover, evolutions of MeOH and DMDS yields with time on stream and temperature were very different. These observations suggest that different catalytic sites exist on the γ-MnO_2 catalytic surface. Furthermore, the products were not detected immediately at the beginning of the reaction but after a latent period depending on the temperature. Additional results[60] have also shown that this latent period was also dependent on the methanethiol concentration. The catalyst modifications undergone by γ-MnO_2 and occurring during the reaction are therefore supposed to have a promoting effect on these products' formation. The relations existing between the catalyst modifications and the product formation are considered below.

a. Dimethyl Disulfide. Figure 2 shows that dimethyl disulfide appeared after a certain reaction period. This reaction period was found to be shortened with increasing methanethiol concentration.[60] Modifications of the γ-MnO_2 sample are thus thought to be necessary to the appearance of dimethyl disulfide in the stream. Higher yields of DMDS were observed when the reactions were performed at 260 and 280 °C. Moreover, dimethyl disulfide was produced in large yield over Mn_2O_3 and started to form on this solid as soon as the reaction with methanethiol began (Figure 5). An important reduction of the manganese oxidation state was detected over the catalysts after reaction at 260 and 280 °C. The formation of dimethyl disulfide is thus assumed to be enhanced on reduced manganese sites where the oxygen supply is decreased. Because less oxygen is consumed by reaction 1 than by the complete oxidation of methanethiol to H_2O, CO_2, and SO_x, the formation of incomplete oxidation products such as dimethyl disulfide seems to be promoted by the reduced oxygen mobility of these catalytic sites. In a previous study, we have shown that dimethyl disulfide was also formed over the manganese sulfate samples but only at 280 °C.[20] The dehydration of the manganese sulfate has been demonstrated to occur at this temperature. The formation of dimethyl disulfide therefore also seems to happen on the dehydrated manganese sulfate phase, which is also formed at 260 and 280 °C. In the low-temperature region (below 200 °C), the formation of dimethyl disulfide is thus assumed to be favored by the reduction of manganese oxide (i.e., lower oxygen mobility). In the higher-temperature region, both the reduction and the formation of the anhydrous manganese sulfate phase can induce the formation of dimethyl disulfide.

b. Methanol. As for dimethyl disulfide, the formation of methanol was delayed with regard to the beginning of the reaction, but the latent period required before the appearance of methanol was shorter than the one observed for dimethyl disulfide. Ross and Sood[29] have reported that the presence of water in the reactant flow increased the methanol production over a cobalt molybdate catalyst. Moreover, they explained the formation of CH_3OH as an interaction of CH_3- species with hydroxyls of the catalyst. The following reaction of hydration could explain the results: $CH_3SH + H_2O \rightarrow CH_3OH + H_2S$ (2). The water required to accomplish this reaction would be produced by the other oxidation reactions. However, the formation of SO_x species is much more favorable than the formation of more reduced H_2S species in the oxidizing atmosphere encountered in the studied reaction. A thermodynamic calculation confirms that the reaction $CH_3SH + H_2O \rightarrow CH_3OH + H_2S$ (2) ($\Delta G = 44$ kJ at 150 °C) is less favored than the oxidation reaction $CH_3SH + \{(1 + x)/2\}O_2 \rightarrow CH_3OH + SO_x$ (3) ($\Delta G = -441$ or -500 kJ at 150 °C) regardless of the formation of SO_2 or SO_3.[61] A reaction initiated by an oxidative

cleavage of the C−S bond resulting in CH_3- species and the oxidation of the sulfur to SO_x species seems therefore most probable. Over the manganese sulfate sample, we have shown that the formation of CH_3OH is enhanced at low temperature (150 and 220 °C) and suppressed at 280 °C when the sulfate dehydrates.[17] Moreover, we also demonstrated that oxygen is absolutely necessary to convert methanethiol and to form methanol even if water vapor is added to the feed flow.[20] Although discrepancies regarding the exact structure of $MnSO_4 \cdot H_2O$ and the presence of real crystallization water exist in the literature,[62−64] hydroxyl groups bound to the sulfur atom are assumed to be present in the hydrated form of manganese sulfate. This hypothesis agrees with the observations of Lendormy,[62] who stated the existence of "SO_5H_2" groups rather than the coexistence of SO_4^{2-} groups and crystallographic water molecules. Moreover, our DRIFTS study has indicated that sulfate species are in a hydrated form as evidenced by the shift of the sulfate band with respect to its usual position. We can make the assumption that these hydroxyl groups present on the sulfur atom are labile and would participate in the formation of the methanol. At higher temperature, the $MnSO_4 \cdot H_2O$ phase is not stable anymore, and the anhydrous $MnSO_4$ phase is formed. This phase does not contain labile hydroxyl groups anymore and is therefore less reactive toward the formation of CH_3OH and the conversion of methanethiol. The formation of methanol is thus assumed to result from the interaction of CH_3- species (coming from an oxidative cleavage of the CH_3SH molecules) with hydroxyl species present on the surface of the hydrated sulfated γ-MnO_2 catalyst.

V. Conclusions

This work has shown that the activity of γ-MnO_2 is strongly influenced by the reaction with methanethiol. Combinations of XPS, XRD, DRIFTS, and potentiometric analyses of various samples characterized after reactions performed under different reaction conditions have allowed us to distinguish between two domains of temperature corresponding to two different behaviors. These two temperature regions are characterized by the formation of different types of sulfate species that influence the catalyst activity and the formation of organic byproducts. At rather low temperature (below 200 °C), adsorbed sulfate species (sulfuric acid-like species) accumulated on the catalyst surface and inhibited the further adsorption and conversion of methanethiol. At higher temperature (260 and 280 °C), the catalyst was greatly reduced and transformed into a bulk manganese phase. As previously observed with manganese sulfate, the activity of the in situ-formed manganese sulfate phase appears to be strongly dependent on the reaction temperature. Indeed, whereas an increase in the reaction temperature provokes its dehydration and associated deactivation, a decrease in the temperature induces activation through the hydration of the manganese sulfate phase. The variations of reaction temperature between 280 and 150 °C dictate the hydration state of the manganese sulfate phase and also induce an important change in the production of the main organic byproducts (methanol and dimethyl disulfide). Methanol is promoted on the hydrated phase maintained only in the lower-temperature region. However, the formation of dimethyl disulfide is enhanced by the dehydration of the manganese sulfate phase at higher temperature.

Acknowledgment. Mrs. M. F. Piton and Erachem Europe S.A. (Tertre, Belgium) are gratefully acknowledged for providing the manganese oxides and performing the manganese potentiometric titration measurements. We also thank the Région Wallonne (convention 971/3667) and the Fonds National de la Recherche Scientifique of Belgium (FNRS) for their financial support.

References and Notes

(1) Prasad, R.; Kennedy, L. A.; Ruckenstein, E. *Catal. Rev.—Sci. Eng.* **1984**, *26*, 1.
(2) Spivey, J. J. *Ind. Eng. Chem. Res.* **1987**, *26*, 2165.
(3) Lahousse, C.; Bernier, A.; Grange, P.; Delmon, B.; Papaefthimiou, P.; Ioannides, T.; Verykios, X. *J. Catal.* **1998**, *178*, 214.
(4) Gandia, L. M.; Gil, A.; Korili, S. A. *Appl. Catal. B* **2001**, *33*, 1.
(5) Baldi, M.; Sanchez-Escribano, V.; Gallardo-Amores, J. M.; Milella, F.; Busca, G. *Appl. Catal. B* **1998**, *17*, L175.
(6) Wang, X.; Xie, Y.-c. *React. Kinet. Catal. Lett.* **2000**, *71*, 263.
(7) Finocchio, E.; Busca, G. *Catal. Today* **2001**, *70*, 213.
(8) Ferrandon, M.; Carno, J.; Jaras, S.; Bjornborn, E. *Appl. Catal. A* **1998**, *180*, 153.
(9) Kijlstra, W. S.; Biervliet, M.; Poels, E. K.; Bliek, A. *Appl. Catal. B* **1998**, *16*, 327.
(10) Brueckner, A.; Bentrup, U.; Radnik, J.; Richter, M.; Fricke, R. *Stud. Surf. Sci. Catal.* **2003**, *145*, 463.
(11) Shelef, M.; Otto, K.; Otto, N. C. *Adv. Catal.* **1978**, *27*, 311.
(12) Tsyrulnikov, P. G.; Kovalenko, O. N.; Gogin, L. L.; Starostina, T. G.; Noskov, A. S.; Kalinkin, A. V.; Krukova, G. N.; Tsybulya, S. V.; Kudrya, E. N.; Bubnov, A. V. *Appl. Catal. A* **1998**, *167*, 31.
(13) Spivey, J. J.; Butt, J. B. *Catal. Today* **1992**, *11*, 465.
(14) Oudar, J. *Catal. Rev.—Sci. Eng.* **1980**, *22*, 171.
(15) Lee, J. H.; Trimm, D. L. *Fuel Process. Technol.* **1995**, *42*, 339.
(16) Heyes, C. J.; Irwin, J. G.; Johnson, H. A.; Moss, R. L. *J. Chem. Technol. Biotechnol.* **1982**, *32*, 1025.
(17) Sultanov, M. Yu.; Al'tshel, I. S.; Makhmudova, Z. Z. *Kinet. Catal.* **1987**, *28*, 213.
(18) Gandia, L. M.; Korili, S. A.; Gil, A. *Stud. Surf. Sci. Catal.* **2002**, *143*, 527.
(19) Heyes, C. J.; Irwin, J. G.; Moss, R. L. *J. Chem. Technol. Biotechnol.* **1985**, *35A*, 89.
(20) Cellier, C.; Gaigneaux, E. M.; Grange, P. *J. Catal.* **2004**, *222*, 255.
(21) Wang, C. H.; Weng, H. S. *J. Chin. Inst. Chem. Eng.* **1998**, *29*, 121.
(22) Wang, C. H.; Weng, H. S. *Ind. Eng. Chem. Res.* **1998**, *37*, 1774.
(23) Ishikawa, A.; Komai, S.; Satsuma, A.; Hattori, T.; Murakami, Y. *Appl. Catal., A* **1994**, *110*, 61.
(24) Otsuka, K.; Tanaka, K.; Morikawa, A. *Bull. Chem. Soc. Jpn.* **1979**, *52*, 2069.
(25) Otsuka, K.; Tanabe, T.; Morikawa, A. *J. Catal.* **1977**, *48*, 333.
(26) Rosso, I.; Garrone, E.; Geobaldo, F.; Onida, B.; Saracco, G.; Specchia, V. *Appl. Catal., B* **2001**, *30*, 61.
(27) JCPDS International Centre for Diffraction Data, 1999.
(28) Dalai, A. K.; Tollefson, E. L.; Yang, A.; Sasaoka, E. *Ind. Eng. Chem. Res.* **1997**, *36*, 4726.
(29) Ross, R. A.; Sood, S. P. *Ind. Eng. Chem. Prod. Res. Dev.* **1977**, *16*, 147.
(30) Pope, D.; Walker, D. S.; Moss, R. L. *Atmos. Environ.* **1978**, *12*, 1921.
(31) Chu, H.; Horng, K. *Sci. Total Environ.* **1998**, *209*, 149.
(32) Lecomte, M.; de Gunzbourg, J.; Teyrol, M.; Miedan-Gros, A.; Allain, Y. *Solid State Commun.* **1972**, *10*, 235.
(33) Maskell, W. C.; Shaw, J. A. E.; Tye, F. L. *Electrochim. Acta* **1981**, *26*, 1403.
(34) Maskell, W. C.; Shaw, J. A. E.; Tye, F. L. *J. Appl. Electrochem.* **1982**, *12*, 101.
(35) Moulder, J. F.; Stickle, W. F.; Sobol, P. E.; Bomben, K. D. *Handbook of X-ray Photoelectron Spectroscopy*; Perkin-Elmer: Eden Prairie, MN, 1992.
(36) Kim, M. H.; Nam, I.-S.; Kim, Y. G. *J. Catal.* **1998**, *179*, 350.
(37) Yu, X.-R.; Liu, F.; Wang, Z.-Y.; Chen, Y. *J. Electron Spectrosc. Relat. Phenom.* **1980**, *50*, 159.
(38) Strohmeier, B. R.; Hercules, D. M. *J. Phys. Chem.* **1984**, *88*, 4922.
(39) van der Heide, H.; Hemmel, R.; van Bruggen, C. F.; Haas, C. *J. Solid State Chem.* **1980**, *33*, 17.
(40) Dijs, I. J.; Jenneskens, L. W.; Geus, J. W. *Stud. Surf. Sci. Catal.* **2002**, *143*, 803.
(41) Veal, B. W.; Paulikas, A. P. *Phys. Rev. Lett.* **1983**, *51*, 1995.
(42) Shirley, D. A. *Phys. Scr.* **1975**, *11*, 117.
(43) Cellier, C.; Baudelet, M.; Ruaux, V.; Lahousse, C.; Gaigneaux, E. M.; Grange, P. To be submitted for publication.
(44) Lahousse, C.; Cellier, C.; Delmon, B.; Grange, P. *Stud. Surf. Sci. Catal.* **2000**, *130*, 587.

(45) Ardizzone, S.; Bianchi, C. L.; Signoretto, M. *Appl. Surf. Sci.* **1998**, *136*, 213.
(46) Paál, Z.; Wild, U.; Muhler, M.; Manoli, J.-M.; Potvin, C.; Buchholz, T.; Sprenger, S.; Resofszki, G. *Appl. Catal. A* **1999**, *188*, 257.
(47) Buchholz, T.; Wild, U.; Muhler, M.; Resofszki, G.; Paál, Z. *Appl. Catal. A* **1999**, *189*, 225.
(48) Buciuman, F.; Pactas, F.; Craciun, R.; Zahn, D. R. T. *Phys. Chem. Chem. Phys.* **1999**, *1*, 185.
(49) Bensitel, M.; Saur, O.; Lavalley, J.-C.; Mabilon, G. *Mater. Chem. Phys.* **1987**, *17*, 249.
(50) Laperdrix, E.; Sahibed-dine, A.; Costentin, G.; Saur, O.; Bensitel, M.; Nédez, C.; Saad, A. B. M.; Lavalley, J. C. *Appl. Catal. B* **2000**, *26*, 71.
(51) Bensitel, M.; Saur, O.; Lavalley, J. C.; Morrow, B. A. *Mater. Chem. Phys.* **1988**, *19*, 147.
(52) Saur, O.; Bensitel, M.; Saad, A. B. M.; Lavalley, J. C.; Tripp, C. P.; Morrow, B. A. *J. Catal.* **1986**, *99*, 104.
(53) Babou, F.; Coudurier, G.; Vedrine, J. C. *J. Catal.* **1995**, *152*, 341.
(54) Moreno, J. A.; Poncelet, G. *Appl. Catal. A* **2001**, *210*, 151.
(55) Ohnishi, R.; Matsui, A.; Tanabe, K. *Bull. Chem. Soc. Jpn.* **1974**, *47*, 2595.
(56) *CRC Handbook of Chemistry and Physics*, 64th ed.; Weast, R. C., Ed.; CRC Press: Boca Raton, FL, 1981.
(57) Mars P.; van Krevelen, D. W. *Chem. Eng. Sci.* **1954**, *3*, 41.
(58) Liao, P.-C.; Fleisch, T. H.; Wolf, E. E. *J. Catal.* **1982**, *75*, 396.
(59) Farrauto, R. J.; Wedding, B. *J. Catal.* **1973**, *33*, 249.
(60) Cellier, C. Ph.D. Thesis, Catholic University of Louvain, Louvain-la-Neuve, Belgium, 2003.
(61) Talonen, T.; Eskelinen, J.; Syvajarvi, T.; Roine, A. *Program HSC: Developed for Thermodynamic Calculations*, version 4.1; Outokumpu Research: Finland, 1999.
(62) Lendormy, N. *Chim. Anal.* **1962**, *44*, 255.
(63) Le Fur, Y.; Coing-Boyat, J.; Bassi, G. *C. R. Acad. Sci. Paris, Ser. C.* **1966**, *262*, 623.
(64) Kemmit, R. D. W. *Comprehensive Inorganic Chemistry*, 1st ed.; Pergamon Press: Elmsford, NY, 1973; p 831.